Prevention of Lean Flame Blowout Using a Predictive Chemical Reactor Network Control

Saurabh Gupta, Philip Malte, Steven L. Brunton, Igor Novosselov[1]

ABSTRACT

Optimization of efficiency and pollution control for gaseous species and particulate matter are common to any combustion system. Combustor lean blowout (LBO) is a concern for aircraft safety and for land-based gas turbines designed to operate at lean equivalence ratios to achieve better fuel efficiency and to limit NO_x emissions. This paper provides an experimental demonstration of model-based control applied to a laboratory jet-stirred reactor (JSR) approaching LBO. The approach uses (1) combustor temperature measurements, coupled with (2) the calculation of free radical concentrations in the reactor using a real-time chemical reactor network (RT-CRN) model as the reactor approaches LBO, which in turn (3) are used by a predictive control algorithm to achieve stable combustion. The RT-CRN represents the combustor as three perfectly stirred reactors (PSRs) in series with a recirculation pathway; the model inputs include real-time measurements of temperature and mass flow rates of fuel and air. In a series of experiments, the combustor is operated on a premixed methane-air mixture; after achieving stable combustion, the air flow rate is increased beyond the stable air-fuel ratio either as a step function or by ramping up linearly. The predictive RT-CRN control algorithm calculates the distribution of hydroxyl (OH) radicals in the free jet, impinging jet, and recirculation regions of the JSR in near real-time (~1 sec delay), and determines the leanest stable state based on the OH uniformity in the combustor. As the OH shifts towards the recirculation region, the reactor approaches LBO, if this condition is detected the control algorithm injects additional fuel; reactor stabilization is achieved within a 5-15 second time frame. Although this proof-of-concept demonstration is performed for LBO control in a JSR with ceramic walls, the control methodology is applicable to other types of high-intensity recirculation stabilized combustors.

BACKGROUND AND RELEVANCE

Lean flame blowout (LBO) can be defined as the phenomenon of flame extinction due to the reduction of the fuel-air ratio beyond a minimum threshold limit at which a given geometry can sustain a flame. The NO_x and soot emissions can be

[1] Corresponding author ivn@uw.edu, Department of Mechanical Engineering, University of Washington

controlled by lowering the flame temperature through leaning of the flame fuel-air equivalence ratio (Φ). However, by operating very lean, the combustors have limited margins between stable combustion and lean-flame instabilities leading to lean blowout. Lean-premixed concepts have been investigated by several aircraft engines developers [1, 2], where the flame instability and extinction is a primary safety concern. Owing to the expensive and potentially dangerous implications, predicting and preventing LBO is of considerable interest to researchers and practitioners. Blowout has mainly been studied in terms of the residence time of reactants [3-5] and flame structures and corresponding strain rates [6, 7]. The Damkohler number (Da) is used for LBO characterization; it is defined as the ratio of mixing time to the chemical time (τ_{mix}/τ_{chem}). For aerodynamically stabilized reactors, blowout occurs when the rate of entrainment of reactants into the recirculation zone cannot be balanced by the rate of their consumption [8]. *Da* non-uniformity can also lead to the onset of flow instabilities resulting in LBO [9]. Experimental and numerical studies have investigated species distribution in different combustor geometries, injector designs and fuel compositions e.g., [10-17]. The CFD models are computationally intensive and cannot be used for real-time calculations. Recently, fast phenomenological CRN and semi-empirical approaches [18, 19] for aero-engine LBO prediction have been proposed.

Flame stabilization has been attempted using a variety of techniques - equivalence ratio modulation, fuel flow redistribution inside the combustor, usage of a secondary fuel, etc. These controllers can be classified based on if the controller injects energy into the system (active vs. passive) and if measurement data from the system is fed back to modulate the control signal (closed-loop vs. open-loop). Combustion control has been extensively studied in the literature [20], especially as it relates to fluid flow control [21-23]. Both, operating point control (OPC) and active combustion control (ACC) [24] have been proposed. In the OPC approach, the system maintains a certain flame parameter within an operating limit while in ACC, the objective is to limit combustion instabilities or to improve the combustion characteristics. Model-based feedback uses measurement in conjunction with a transfer function or a state-space model to determine an appropriate control signal. System identification, such as the eigensystem realization algorithm [25, 26], yields linear reduced-order models that have been used to control cavity flow and combustion oscillations. Morgans and Dowling [27] used an open-loop transfer function (OLTF) to control thermo-acoustic instabilities in a Rijke tube experiment and in an atmospheric pressure combustor. Campos-Delgado et al. [28] tested model-based control of thermo-acoustic instabilities in a swirl-stabilized spray combustor using linear-quadratic-Gaussian (LQG) control, loop transfer recovery (LTR), and H_∞ loop-shaping. Some examples of model-based boiler control include artificial neural networks (ANN) [29] and model predictive

control (MPC) [30]. In addition to the various model-based control strategies, there are also numerous studies that employ model-free control. The most common model-free combustion control is extremum-seeking control (ESC) [31], where a sinusoidal perturbation is added to the control signal to estimate the gradient of an objective function for optimization. ESC has been used to control thermoacoustic modes in an industrial scale 4MW gas turbine combustor by Banaszuk et al. [32, 33]. Kalman filters were later combined with ESC for dramatic performance improvement in thermoacoustic instability control in a combustor experiment by Gelbert et al. [34]. ESC was also used earlier to tune PI controllers to stabilize a nonlinear acoustic oscillation model of a combustion chamber by Krstic et al. [35]. Other model-free strategies include the use of evolutionary algorithms to optimize noisy combustion processes by Buche et al. [36]. These methods were also used to tune the parameters of a model-based H_∞ controller in a combustion experiment by Hansen et al. [37].

EXPERIMENTAL SETUP

The experimental setup uses an atmospheric pressure, single-jet JSR, fired on methane. JSRs provide a strongly recirculating combustion field that fills much of the reactor. This environment is useful for studying chemical-kinetic driven effects that are relevant to practical, high-intensity, back-mixed combustion systems, especially the primary combustion zone of gas turbine engines. Two of these effects are blowout and NOx formation. The original stirred reactor of Longwell and Weiss [3] was developed to study the problem of engine blowout. Later, JSRs were used to study NOx formation and reduction in lean-premixed combustors, e.g., [38].

The total volume of the reaction chamber of the JSR used here is 15.8 cm^3. The walls of the JSR are ceramic (cast from alumina, Al_2O_3). The balance of the JSR setup consists of a stainless steel premixer/injector manifold and an Inconel nozzle block, seeFigure 1. The flow rates of air and fuel into the premixer are controlled by two mass-flow controllers (MFCs) operated by National Instruments MyRio module via a LabVIEW environment. The air is supplied from the filtered shop airline regulated at 50 psig at the inlet of the MFC. The fuel is supplied from a high-pressure cylinder, again regulated to a pressure of 50 psig upstream of the MFC. Under all air/fuel flow rates, the air-fuel premix enters the reactor cavity through a 2 mm nozzle at sonic velocity. Temperature in the recirculation zone is measured using an R-type thermocouple (TC), with an alumina coating to prevent catalytic effects. The thermocouple data is relayed to the LabVIEW interface using a TC-DAQ (Omega Systems).

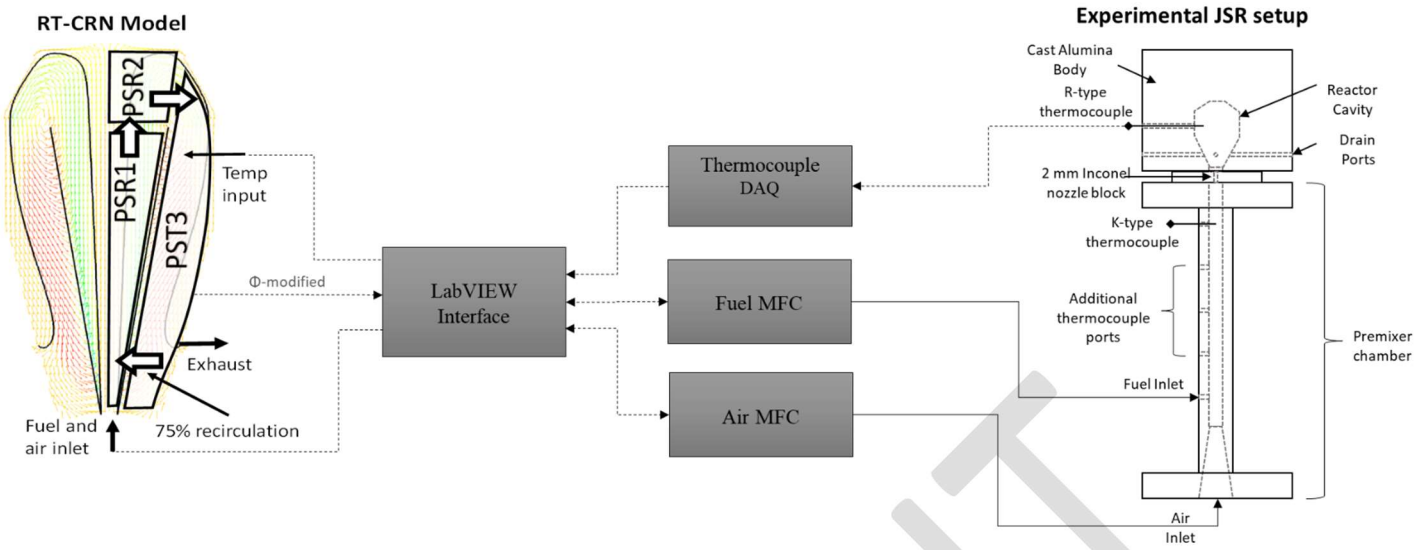

Figure 1: Schematic diagram of the control approach. The reactor operational condition is disturbed by a sudden or gradual increase in the air flow rate. Experimental temperature measurements are used as input to the CRN that continuously calculates species distribution in the reactor in real-time. The output of the CRN model is then used by the control algorithm to estimate proximity to LBO and to update the fuel flow rate required to achieve a stabilizing equivalence ratio.

COMPUTATIONAL MODEL

CRN models have been used to study blowout and pollutant formation in laboratory reactors and gas turbine engines, e.g. [18, 38-47]. Recently, Kaluri et al. [48] reported model-based monitoring and real-time prediction of LBO for the present JSR. The approach used combustion temperature measurements, coupled with the RT-CRN to interpret the data as it is collected, see Figure 1. The jet-flame region is modeled as an adiabatic PSR1 with relatively small volume. The jet impinging region, i.e., a near post-flame zone, is modeled as PSR2. The recirculation zone is modeled as an assigned (i.e., measured) temperature stirred reactor (PST3), owing to the heat transfer from the burning gases to the reactor walls. The three reactors cover the full volume of the JSR. The temperature input is provided by the R-type thermocouple measurements. During the transition from higher to lower Φ, the reactor wall is hotter than the gas, resulting in heat transfer into the system. The volumes and the flow splits of the individual CRN elements are determined based on the CFD solution of Karalus [47]. The single-jet JSR used in this study has a recirculation ratio of 75%; that is, the average fluid particle passing through the JSR makes four passes through the reactor before being exhausted based on the jet entrainment calculation [49-51], and later confirmed by CFD modeling [52, 53]. The CRN configuration is based on the reactor behavior under stable combustion (T >1700K). The time-dependent trends for the predicted free radical concentrations in each CRN element are available with a time resolution of ~1 sec. The CRN code used here is developed in-house [54, 55]. One of the major advantages of this code is in the implementation of the fast convergence algorithm,

which enables near-real-time chemical kinetic calculations in complex CRN arrangements [56, 57]. In this work, a detailed chemical kinetic mechanism GRI 3.0 is used [58].

CONTROL ALGORITHM

The control algorithm is based on time-resolved trends of OH concentrations during transient combustor operation, i.e., as the rector cools, the peak OH concentration (thus, the flame) moves downstream. The work of Karalus et al [59, 60] is basis of using the OH as a parameter for the control methodology; CFD and CRN modeling was used to examine the behavior of the active species chain carriers (H, O, and OH) as the combustion gas flowed through the JSR, from the jet flame (PSR1), to the jet impingement zone (PSR2), to the recirculation zone (PSR3). As the fuel-air equivalence ratio was decreased from that corresponding to lean combustion at 1800 K to lean blowout, the active species were found to be delayed in their peak concentrations to later convective times as phi was decreased. As the JSR approached lean blowout, the induction time from get inlet to the peak in H-atom concentration increased and OH was the longest surviving active species. The amount of OH remaining late in the flow cycle around the JSR and available for entrainment into the jet appeared to play a key role in maintaining ignition [48]. Thus, our work has focused on using OH as the control parameter and comparing its behavior in the zones of the JSR as lean blowout is approached. The active species are known to be essential for ignition and OH is known to remain into the near post-flame region [61, 62]. The RT-CRN model [63], shown in Figure 1, compares the OH radical concentrations in the different reactor zones, and the ratio of OH concentrations in the jet-flame zone to the recirculation zone is used as a criterion for the LBO proximity. Three distinct evePnts are shown during the reactor transition from a stable operating condition to LBO: Event-1: OH radical concentration in PSR1 drops steadily and decreases to a value equal to OH radical concentration in PST3 (OH concentration is nearly uniform in the JSR); Event -2: OH radical concentration in PSR1 drops abruptly (blowout in jet-flame region); Event-3: OH radical concentration in PSR2 drops abruptly below that in PST3 (global LBO). In the current work, the primary objective of the control algorithm is to operate the reactor at the lowest stable Φ, i.e., at closest to uniform OH concentration. Thus, the computed OH ratio of PSR1/PSR3 (*rOH*) of unity is used as the operating set point. For operational stability, a tolerance of 5% is considered acceptable (*rOH*=1±0.05). At all values of *rOH* <0.95, the control algorithm increases the fuel flow based on the protocol defined in Table 1. As the fuel flow increases, the flame moves upstream, and the *rOH* >1.05 condition may be reached; in this case, the algorithm reduces the fuel flow to prevent significant overshoot, and a damping factor of 0.25 is used. During the stable operating condition *rOH* >1.2, the control algorithm monitors the OH concentration but does not interfere with the

combustor operation; this condition is observed before the initial disturbance occurs. The conditions where air flow was decreased were not tested.

Table 1: Control Algorithm

OH ratio (rOH_k)	Modified Φ
$rOH_k < 0.5$	$\Phi_{k+1} = \Phi_k + 0.1$
$0.5 \leq rOH_k < 0.95$	$\Phi_{k+1} = \Phi_{k-1} + (\Phi_k - \Phi_{k-1}) * \frac{1 - rOH_{k-1}}{rOH_k - rOH_{k-1}} * 0.25$
$0.95 \leq rOH_k \leq 1.05$	$\Phi_{k+1} = \Phi_k$
$1.05 < rOH_k < 1.2$	$\Phi_{k+1} = \Phi_{k-1} + (\Phi_k - \Phi_{k-1}) * \frac{1.1 - rOH_{k-1}}{rOH_k - rOH_{k-1}} * 0.25$
$rOH_k \geq 1.2$	$\Phi_{k+1} = \Phi_k$

The overall control architecture is described in Algorithm 1.

Algorithm 1: Control algorithm

$\Phi_{k+1} = updateControl()$
% Symbols:
% Φ_{k+1}: Output equivalence ratio control signal from algorithm to system
% Φ_k: Equivalence ratio of the system at the beginning of current computation cycle
% Φ_{k-1}: Equivalence ratio of the system at the beginning of previous computation cycle
% rOH_k: OH ratio at the beginning of current the computation cycle
% rOH_{k-1}: OH ratio at the beginning of previous computation cycle
begin
T = recordExperimentalTemperature(); *% experimental measurements of temperature*
rOH_k = runCRN(T); *% compute rOH from CRN model*
$\Phi_{k+1} = \text{computePhi}(\Phi_k, \Phi_{k-1}, rOH_k, rOH_{k-1})$; *% update equivalence ratio (control input)*
setFuelMFC(Φ_{k+1}); *%enact updated Φ via fuel MFC*
end

RESULTS AND DISCUSSIONS

In the current work, the air flow rate is the independent variable; the fuel flow is used as the actuator, adjusting Φ to prevent LBO. The initial condition is: air flow =0.8 g/s, Φ=0.75. Once a steady-state condition (steady temperature) is achieved, the air flow rate is changed, the controller is used to stabilize the system under the new air flow. Two scenarios are investigated.

1. Step function air flow rate increase

In Set#1, the air flow is increased as a step function from 0.8 g/s to a higher value that would result in flame extinction. Table 2 shows the initial conditions and the controlled performance for three different final air flow rates. The response time is defined as the time period between the initial increase in the air flow rate and the start of the fuel flow rate increase. Since this experiment involves an instantaneous increase in the air flow rate, the initial response time is approximately the

same for all cases and is a function of several hardware related delays, e.g., a thermocouple and fuel MFC responses, as well computational delay related to CRN convergence, which depends on the stiffness of the numerical problem and the initial guess values (1-5 seconds near LBO and less than 0.1 seconds during stable operation).

The stabilization time is the time required to bring the system to a stable condition after the initial change in the air flow rate. The stable condition is identified when a stable value of *rOH* = 1.00 ± 0.05 (0.95-1.05) is reached. After OH stabilization, the experimental parameters, such as equivalence ratio and temperature, can change as the reactor continues to cool down, which typically takes 15-20 minutes due to the high thermal inertia of the ceramic walls [63]. The control algorithm is able to track this slow cool down keeping the *rOH* value within the operational set point range. Table 2 shows that the mean values of the experimental Φ for the stabilized condition are similar for all cases; however, the difference in the air flow rates, and thus the reactor residence times, results in differences in the mean stable temperature values.

Table 2: Cases for the experiment set# 1: step function airflow increase, Initial flow air flow rate is 0.8 g/s.

	Final air flow rate (g/s)	Initial response time (sec)	Stabilization time (sec)	Mean OH ratio under stable condition	Mean Φ, stabilized condition	Mean exp. temp. stabilized condition (K)
Case 1	1.0	15	72	0.952	0.62	1575
Case 2	1.2	15	46	0.993	0.61	1630
Case 3	1.3	15	46	0.965	0.62	1641

Figure 2 depicts the typical system, Set#1 Case#2 is shown. At time = 0 sec, the air flow rate is increased as a step function from 0.8 to 1.2 g/s; the fuel flow is kept constant resulting in an instantaneous reduction of Φ from 0.75 to 0.5 which is not a stable operating condition for the reactor operating on methane [63]. The measured temperature in the recirculation zone and thus the input to PST3 drops from 1750K to 1550K within the first 15 seconds. The temperature data shown are the raw thermocouple readings, uncorrected for the radiative heat loss from the thermocouple, which is estimated to vary from 25K to 40K as the gas temperature increases from 1500K to 1750K. The CRN calculates conditions in the reactor zones in near-real time. For PSR1, the calculated temperature decreases to about 1300K, and the calculated OH concentration drops significantly (*rOH* → 0): PSR1 has blown out. The control algorithm increases the fuel flow rate in response to the rOH (below 0.5); the fuel flow is increased as $\Phi_{k+1} = \Phi_k + 0.1$. Over the next minute, the algorithm adjusts the fuel input based on the calculated rOH values. Oscillating behavior of temperature and chemical species is dampened overtime as the system adjusts to the new conditions. Here, adjustments to the step size and the damping factor may yield faster stabilization, significant tuning of the coefficients has not been performed in these proof-of-concept experiments.

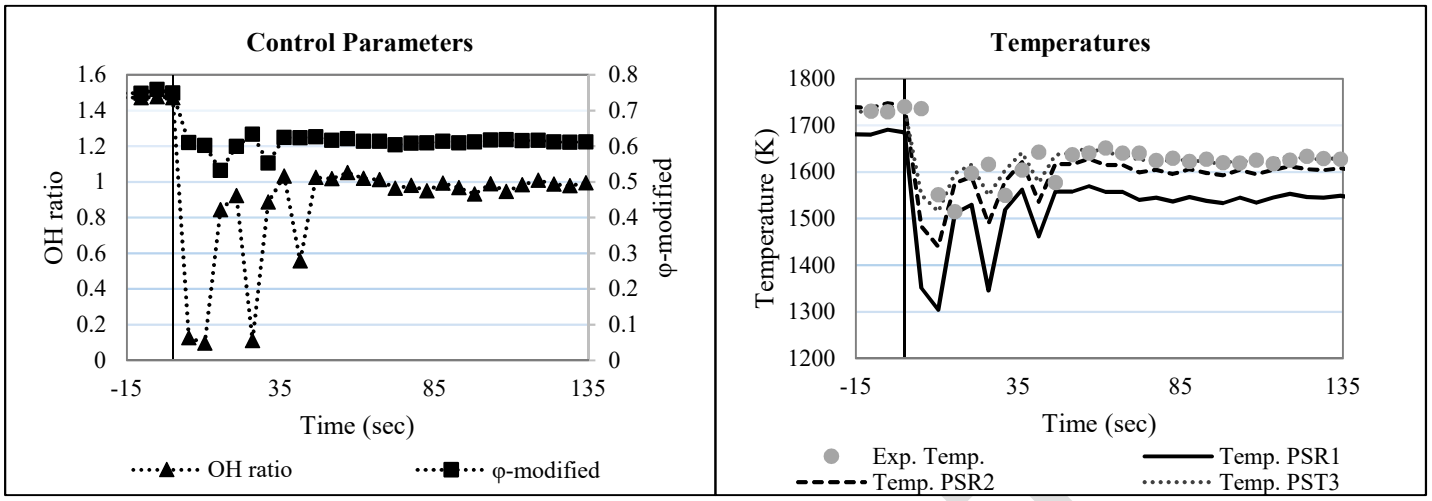

Figure 2: Set #1, case #2 reactor stabilization as a response to step function change in air flow from 0.8 to 1.2 g/s. Left: Calculated OH ratio and Φ, Right: Measured and calculated temperatures

2. Monotonically increasing function for air flow rate

Set#2 is conducted by increasing the air flow as a monotonically increasing function of time, i.e., the air flow rate is ramped-up from 0.8 g/s to 1.2 g/s within a specific period of time as shown in Table 3.

Table 3: Cases for set#2, monotonically increasing air flow. Initial flow air flow rate is 0.8 g/s, final 1.2 g/s.

	Ramp time (sec)	Initial response time (sec)	Stabilization time (sec)	Mean OH ratio under stable condition	Mean Φ stabilized condition	Mean exp. temp. stabilized condition (K)
Case 1	30	26	51	0.985	0.643	1625
Case 2	60	26	56	0.981	0.642	1622
Case 3	120	36	97	0.978	0.642	1621
Case 4	180	51	127	0.977	0.641	1620
Case 5	240	61	179	0.980	0.643	1620
Case 6	360	94	427	1.043	0.641	1635

Figure 3 shows the results for Set#2 Case#4. The control algorithm is again successful in preventing a blowout, and the system is subsequently stabilized. Similar behavior is observed for all cases in Set#2. The major difference from Set#1 experiments is that the measured temperature changes more gradually and the algorithm is able to control the system behavior without significant overshooting, as in the step function disturbance cases. Since the rate of air flow ramp-up decreases from Case#1 to Case#6, the initial response time follows an increasing trend over these cases. The stabilization times also increase as the ramp time increases. The stability criterion is the same as in Set#1, Case#2; however, the stabilization Φ is higher, as the reactor walls cool down further than in the step function experiments. The OH ratio under the stable condition is found to be within the set point range of the algorithm.

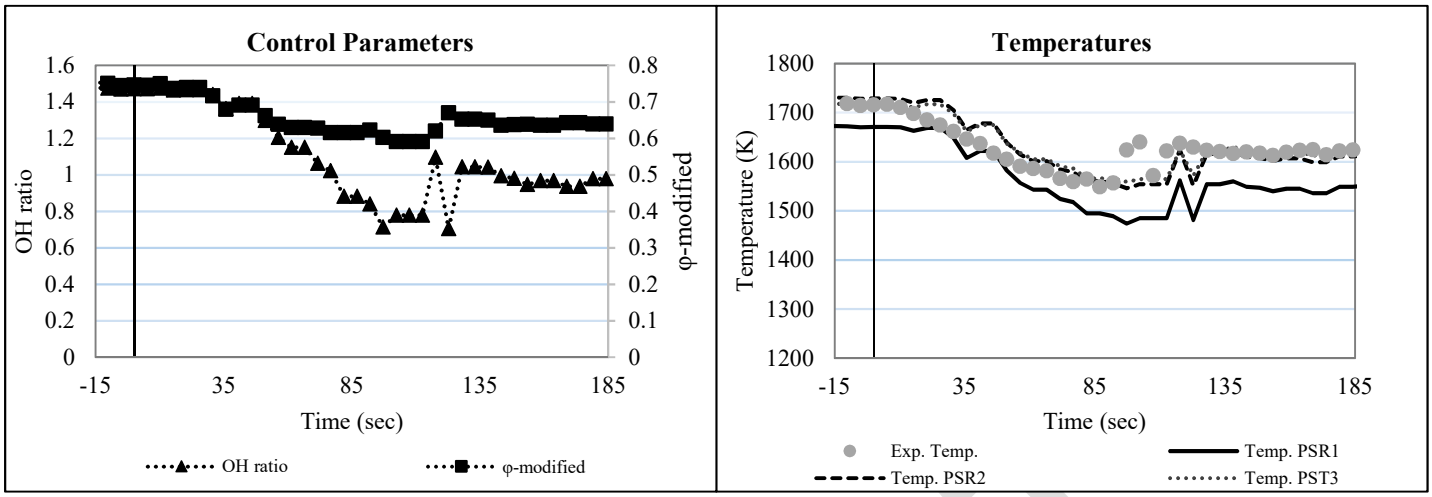

Figure 3: Set #2, case #4 - reactor stabilization as a response to ramp up change in air flow from 0.8-1.2 g/s over 180 seconds. Left - calculated OH ratio and Φ, Right - measured and calculated temperatures

CONCLUSION

This research demonstrates a proof-of-concept of a predictive RT-CRN control methodology for preventing incipient lean blowout. The identification of the onset of a blowout is determined based on the trends of the computed concentrations of a critical combustion species, the OH radical, using a chemical reactor network. A phenomenological three-zone RT-CRN configuration with PSR1 (the jet-flame region), PSR2 (the impinging jet region) and PST3 (the recirculation zone) is used for the computations. The RT-CRN relies on a temperature measurement in the recirculation zone to calculate the species concentrations in the three zones of the JSR. The ratio of the OH radical concentrations in PSR1 to PSR3 is used as a set point by the control algorithm. In the scenario where the air flow increases and the fuel flow remains constant, the computed OH ratio can drop below unity, corresponding to the flame movement from the jet zone into the recirculation zone. This condition eventually leads to global LBO due to the inability of the recirculating flow to anchor the combustion in the impinging cold jet. The algorithm increases the fuel flow to the condition where the OH concentration in the jet zone and the recirculation zone are equal, and the JSR returns to a stable operating condition. The algorithm response time is on the order of 1-15 seconds, including the CRN computation time of 0.1-5 seconds on a 6 gen Intel® Core™ i7 processor. The GRI 3.0 mechanism is used for CRN computations. Calculations slow down when elements approach blow out, as the chemistry becomes stiff. In the future, these calculations may be accelerated using truncated chemistry. Application of this methodology to other systems requires additional investigation. The present approach employs a proportional control; it is possible that more sophisticated control approaches can be used to obtain better results. In addition to LBO control, the model-based approach can be used for different cost functions, such as combustion efficiency and emissions control. The methods do not require significant modifications in the combustor hardware and can be beneficial for several energy

conversion systems, including gas turbine engines, alternative fuel and biofuel-fired systems, gasifiers, etc. In this work, we vary the air flow as an independent parameter, although the suitability of other variables, such as fuel rate and fuel composition, for the purpose, can be investigated. More complex system disturbances need to be investigated. Other actuation mechanisms can also be used, for example, primary or secondary air flow rates or secondary fuel injection can be adjusted based on the real-time algorithm calculations. In addition, a CRN model may be used in the future for a model predictive control [64, 65], although this requires extremely fast model predictions, as the model is used iteratively inside of an optimization loop.

REFERENCES

1. Liu, Y., et al., *Review of modern low emissions combustion technologies for aero gas turbine engines.* Progress in Aerospace Sciences, 2017.
2. TACINA, R. *Combustor technology for future aircraft*. in *26th Joint Propulsion Conference*. 1990.
3. Longwell, J.P. and M.A. Weiss, *High Temperature Reaction Rates in Hydrocarbon Combustion.* Industrial and Engineering Chemistry, 1955. **47**(8): p. 1634-1643.
4. Williams, G.C., H. Hottel, and A.C. Scurlock. *Flame stabilization and propagation in high velocity gas streams*. in *Symposium on Combustion and Flame, and Explosion Phenomena*. 1948. Elsevier.
5. Yamaguchi, S., N. Ohiwa, and T. Hasegawa, *Structure and blow-off mechanism of rod-stabilized premixed flame.* Combustion and Flame, 1985. **62**(1): p. 31-41.
6. Chaudhuri, S., et al., *Blowoff dynamics of bluff body stabilized turbulent premixed flames.* Combustion and flame, 2010. **157**(4): p. 790-802.
7. Stöhr, M., et al., *Dynamics of lean blowout of a swirl-stabilized flame in a gas turbine model combustor.* Proceedings of the Combustion Institute, 2011. **33**(2): p. 2953-2960.
8. Longwell, J.P., E.E. Frost, and M.A. Weiss, *Flame stability in bluff body recirculation zones.* Industrial & Engineering Chemistry, 1953. **45**(8): p. 1629-1633.
9. Guan, Y. and I. Novosselov, *Damkohler Number Analysis in Lean Blow-Out of Toroidal Jet Stirred Reactor.* Journal of Engineering for Gas Turbines and Power, 2018. **140**(10): p. 104501.
10. Ceglia, G., et al., *Three-dimensional organization of the flow structure in a non-reactive model aero engine lean burn injection system.* Experimental Thermal and Fluid Science, 2014. **52**: p. 164-173.
11. Malbois, P., et al., *Quantitative measurements of fuel distribution and flame structure in a lean-premixed aero-engine injection system by kerosene/OH-PLIF measurements under high-pressure conditions.* Proceedings of the Combustion Institute, 2018.
12. Malbois, P., et al. *Experimental Investigation With Optical Diagnostics of a Lean-Premixed Aero-Engine Injection System Under Relevant Operating Conditions*. in *ASME Turbo Expo 2017: Turbomachinery Technical Conference and Exposition*. 2017. American Society of Mechanical Engineers.
13. Kahraman, N., S. Tangöz, and S.O. Akansu, *Numerical analysis of a gas turbine combustor fueled by hydrogen in comparison with jet-A fuel.* Fuel, 2018. **217**: p. 66-77.
14. Innocenti, A., et al., *Numerical analysis of the dynamic flame response of a spray flame for aero-engine applications.* International Journal of Spray and Combustion Dynamics, 2017. **9**(4): p. 310-329.
15. Lourier, J.-M., et al., *Scale Adaptive Simulation of a thermoacoustic instability in a partially premixed lean swirl combustor.* Combustion and Flame, 2017. **183**: p. 343-357.
16. Tachibana, S., et al., *Experimental and numerical investigation of thermo-acoustic instability in a liquid-fuel aero-engine combustor at elevated pressure: Validity of large-eddy simulation of spray combustion.* Combustion and Flame, 2015. **162**(6): p. 2621-2637.

17. Lipatnikov, A.N., *Stratified turbulent flames: Recent advances in understanding the influence of mixture inhomogeneities on premixed combustion and modeling challenges.* Progress in Energy and Combustion Science, 2017. **62**: p. 87-132.
18. Innocenti, A., et al., *Turbulent flow-field effects in a hybrid CFD-CRN model for the prediction of NO x and CO emissions in aero-engine combustors.* Fuel, 2018. **215**: p. 853-864.
19. Hu, B., Y. Huang, and J. Xu, *A hybrid semi-empirical model for lean blow-out limit predictions of aero-engine combustors.* Journal of Engineering for Gas Turbines and Power, 2015. **137**(3): p. 031502.
20. Dowling, A.P. and A.S. Morgans, *Feedback control of combustion oscillations.* Annu. Rev. Fluid Mech., 2005. **37**: p. 151-182.
21. Brunton, S.L. and B.R. Noack, *Closed-loop turbulence control: progress and challenges.* Applied Mechanics Reviews, 2015. **67**(5): p. 050801.
22. King, R., *Active Flow Control, Notes on Numerical Fluid Mechanics and Interdisciplinary Design, vol. 95*. 2007, Springer-Verlag.
23. Hathout, J., et al., *Combustion instability active control using periodic fuel injection.* Journal of Propulsion and Power, 2002. **18**(2): p. 390-399.
24. Docquier, N. and S. Candel, *Combustion control and sensors: a review.* Progress in energy and combustion science, 2002. **28**(2): p. 107-150.
25. Illingworth, S.J., A.S. Morgans, and C.W. Rowley, *Feedback control of cavity flow oscillations using simple linear models.* Journal of Fluid Mechanics, 2012. **709**: p. 223-248.
26. Illingworth, S.J., A.S. Morgans, and C.W. Rowley, *Feedback control of flow resonances using balanced reduced-order models.* Journal of Sound and Vibration, 2011. **330**(8): p. 1567-1581.
27. Morgans, A.S. and A.P. Dowling, *Model-based control of combustion instabilities.* Journal of Sound and Vibration, 2007. **299**(1-2): p. 261-282.
28. Campos-Delgado, D., et al., *Active control of combustion instabilities using model-based controllers.* Combustion science and technology, 2003. **175**(1): p. 27-53.
29. Chu, J.-Z., et al., *Constrained optimization of combustion in a simulated coal-fired boiler using artificial neural network model and information analysis ☆.* Fuel, 2003. **82**(6): p. 693-703.
30. Havlena, V.r. and J. Findejs, *Application of model predictive control to advanced combustion control.* Control Engineering Practice, 2005. **13**(6): p. 671-680.
31. Ariyur, K.B. and M. Krstic, *Real-time optimization by extremum-seeking control*. 2003: John Wiley & Sons.
32. Banaszuk, A., et al., *An adaptive algorithm for control of combustion instability.* Automatica, 2004. **40**(11): p. 1965-1972.
33. Banaszuk, A., Y. Zhang, and C.A. Jacobson. *Adaptive control of combustion instability using extremum-seeking*. in *American Control Conference, 2000. Proceedings of the 2000*. 2000. IEEE.
34. Gelbert, G., et al., *Advanced algorithms for gradient estimation in one-and two-parameter extremum seeking controllers.* Journal of Process Control, 2012. **22**(4): p. 700-709.
35. Krstic, M., A. Krupadanam, and C. Jacobson, *Self-tuning control of a nonlinear model of combustion instabilities.* IEEE transactions on control systems technology, 1999. **7**(4): p. 424-436.
36. Buche, D., et al., *Multiobjective evolutionary algorithm for the optimization of noisy combustion processes.* IEEE Transactions on Systems, Man, and Cybernetics, Part C (Applications and Reviews), 2002. **32**(4): p. 460-473.
37. Hansen, N., et al., *A method for handling uncertainty in evolutionary optimization with an application to feedback control of combustion.* IEEE Transactions on Evolutionary Computation, 2009. **13**(1): p. 180-197.
38. Rutar, T. and P.C. Malte, *NOx Formation in High-Pressure Jet-Stirred Reactors with Significance to Lean-Premixed Combustion Turbines.* ASME Journal of Engineering for Gas Turbines and Power, 2002. **124**: p. 776-783.
39. Rubin, P. and D. Pratt, *Zone combustion model development and use: Application to emissions control.* American Society of Mechanical Engineers, 1991: p. 1-41.
40. Fackler, K.B., et al., *NOx behavior for lean-premixed combustion of alternative gaseous fuels.* Journal of Engineering for Gas Turbines and Power, 2016. **138**(4).
41. Rutar, T. and P.C. Malte. *NOx formation in high-pressure jet-stirred reactors with significance to lean-premixed combustion turbines*. in *ASME Turbo Expo 2001: Power for Land, Sea, and Air*. 2001. American Society of Mechanical Engineers.

42. Novosselov, I.V., *Eight-Step Global Kinetic Mechanism on Methane Oxidation with Nitric Oxide Formation for Lean-Premixed Combustion Turbines*. 2002, University of Washington.
43. Fichet, V., et al., *A reactor network model for predicting NOx emissions in gas turbines.* Fuel, 2010. **89**(9): p. 2202-2210.
44. Lyra, S. and R. Cant, *Analysis of high pressure premixed flames using Equivalent Reactor Networks for predicting NOx emissions.* Fuel, 2013. **107**: p. 261-268.
45. Mellor, A., *NOx and CO emissions models for gas-fired, lean premixed combustion turbine: Final report.* Vanderbit University, Nashville, TN, 1996.
46. Karalus, M.F., *An investigation of lean blowout of gaseous fuel alternatives to natural gas*, in *Department of Mechanical Engineering*. 2014, University of Washington.
47. Karalus, M.F., et al., *A skeletal mechanism for the reactive flow simulation of methane combustion*, in *ASME Turbo Expo 2013: Turbine Technical Conference and Exposition*. 2013, ASME: San Antonio, Texas, USA.
48. Kaluri, A., P. Malte, and I. Novosselov, *Real-time prediction of lean blowout using chemical reactor network.* Fuel, 2018. **234**: p. 797-808.
49. Beér, J.M. and N.A. Chigier, *Combustion aerodynamics.* New York, 1972.
50. Thorton, M.M., P.C. Malte, and A.L. Crittenden. *Oxidation of furan and furfural in a well-stirred reactor*. in *Symposium (International) on Combustion*. 1988. Elsevier.
51. Novosselov, I.V., *Chemical reactor networks for combustion systems modeling*. 2006, University of Washington.
52. Fackler, K.B., et al., *Experimental and numerical study of NOx formation from the lean premixed combustion of CH4 mixed with CO2 and N2.* Journal of Engineering for Gas Turbines and Power, 2011. **133**(12): p. 121502.
53. Fackler, K.B., *A study of pollutant formation from the lean premixed combustion of gaseous fuel alternatives to natural gas*. 2012.
54. Pratt, D.T. and J.D. Wormeck, *CREK, Combustion Reaction Equilibrium and Kinetics in Laminar and Turbulent Flows.* Report TEL-76-1, Department of Mechanical Engineering, Washington State University, Pullman, WA, 1976.
55. Pratt, D.T., *Calculation of chemically reacting flows with complex chemistry.* Studies in convection: Theory, measurement and applications, 1977. **2**: p. 191-220.
56. Novosselov, I., et al. *Chemical reactor network application to emissions prediction for industial dle gas turbine*. in *ASME turbo expo 2006: Power for land, sea, and air*. 2006. American Society of Mechanical Engineers.
57. Novosselov, I.V., *Chemical reactor networks for combustion systems modeling*, in *Department of Mechanical Engineering*. 2006, University of Washington.
58. Gregory P. Smith, et al. *GRI-Mech Home Page*. Accessed November 2, 2016; Available from: http://www.me.berkeley.edu/gri_mech/.
59. Karalus, M.F., *An investigation of lean blowout of gaseous fuel alternatives to natural gas*. 2014.
60. Karalus, M.F., et al. *Characterizing the mechanism of lean blowout for a recirculation-stabilized premixed hydrogen flame*. in *ASME Turbo Expo 2012: Turbine Technical Conference and Exposition*. 2012. American Society of Mechanical Engineers.
61. Glassman, I., R.A. Yetter, and N.G. Glumac, *Combustion*. 2014: Academic press.
62. Vijlee, S.Z., I.V. Novosselov, and J.C. Kramlich. *Effects of Composition on the Flame Stabilization of Alternative Aviation Fuels in a Toroidal Well Stirred Reactor*. in *ASME Turbo Expo 2015: Turbine Technical Conference and Exposition*. 2015. American Society of Mechanical Engineers.
63. Kaluri, A., P. Malte, and I. Novosselov, *Real-Time Prediction of Lean Blowout Using Chemical Reactor Network* Fuel, 2018. **Accepted**.
64. Garcia, C.E., D.M. Prett, and M. Morari, *Model predictive control: theory and practice—a survey.* Automatica, 1989. **25**(3): p. 335-348.
65. Camacho, E.F. and C.B. Alba, *Model predictive control*. 2013: Springer Science & Business Media.